

An unusual ruby-sapphire-sapphirine-spinel assemblage from the Tertiary Barrington volcanic province, New South Wales, Australia

F. LIN SUTHERLAND

Mineralogy and Petrology Section, Australian Museum, 6 College Street, Sydney, N.S.W. 2000, Australia

AND

ROBERT R. COENRAADS

Gemmological Association of Australia (N.S.W. Division), 24 Wentworth Avenue, Sydney, N.S.W. 2000, Australia

Abstract

Ruby-sapphire-sapphirine-spinel forms small, corroded, crystalline aggregates in corundum bearing alluvials shed from the Tertiary Barrington basalt shield volcano. Sapphirine is near a 7:9:3 ($\text{MgO-Al}_2\text{O}_3\text{-SiO}_2$) composition and, together with the corundum, shows reaction rims of pleonaste spinel. Spinel in the aggregates has a compositional range Sp 68-73 Hc 27-29 Cm 0-3. The aggregates give new insights into the ruby-sapphire source rocks. Potential origins include metamorphic recrystallization of aluminous material (below 1460°C) or high temperature-high pressure crystallization reactions related to lamprophyric or basaltic magmas (up to 1300°C and 20 kbar). Sapphirine-spinel thermometry suggests final crystallization temperatures for the aggregates around 780 to 940°C and reaction with host magmas at over 1000°C.

The Barrington gemfield includes two distinct corundum suites. One, typical in eastern Australia, is dominated by blue-green, well-crystallized, growth-zoned sapphire, commonly containing rutile silk and Fe-rich spinel inclusions (Hc 51-73, Mt 18-35, Mf 6-8, Usp 2-6). The other, an unusual suite, is dominated by ruby and pastel coloured sapphires, with little crystal shape or growth zonation and restricted mineral inclusions, mostly chromian pleonaste and pleonaste. The ruby-sapphire-sapphirine-spinel aggregates provoke new thoughts on the origin of rubies and sapphires and their indicator minerals in eastern Australian and southeastern Asian volcanic gemfields.

KEYWORDS: ruby, sapphire, sapphirine, xenoliths, xenocrysts, Barrington volcanic province, Australian gemfields, Thailand gemfields.

Introduction

RUBY is a relatively rare gemstone in Australia (Sutherland, 1991; Oliver and Townsend, 1993). Ruby and purple/mauve sapphires, including some facet-grade material, appear in corundum-bearing alluvials, shed from several Cainozoic volcanic fields in eastern Australia, but are only common in a few fields (Table 1). The parent rock for rubies in the eastern Australian basalt fields is unknown, although etched surfaces indicating magmatic corrosion and a spatial association with the volcanic provinces

suggest a genetic relationship. This paper describes the unusual ruby-bearing mineral aggregates, as a source assemblage for rubies shed from the Tertiary Barrington Tops shield volcano. These aggregates were identified in heavy mineral concentrates recovered by Mr A.W. Chubb of Gloucester during prospecting operations at Gloucester Tops in the early 1970s and donated to the Australian Museum (Aust. Museum specimen no. D49689).

Alluvial ruby and accompanying sapphire and zircon appear in many drainages dissecting the Barrington basalt shield, particularly on its eastern

TABLE 1. Ruby and purple, mauve, pink corundum sites, Eastern Australia

Locality	Lat.S, Long.E	Volcanic Province	Comments	Ref
Gloucester Tops- Barrington Tops	31°50'–32°05', 151°20'–151°40'	Barrington, New South Wales	common, up to 50% of alluvial corundum concentrates	1 2
Campbell Ck	16°05', 144°30'	McLean, Qld	also other Palmer River drainage	3
Jordan Ck	17°35', 145°40'	Atherton, Qld	also other Jordan River drainage	3
Lava Plains	18°30', 144°45'	McBride, Qld	also other McBride drainage	3
Cheviot Hills	19°35', 144°10'	Chudleigh, Qld		3
Anakie gemfields	22°15'–23°45', 147°20'–147°50'	Hay, Qld	rare finds, includes ruby - sapphire zoned stones	3
Stanthorpe	28°40', 151°55'	Main Range, Qld	restricted alluvial distribution	3
New England gemfields	30°00'–31°00', 151°00'–152°00'	Central, NSW	rare finds, includes ruby - sapphire zoned stones	4,5
Bingara gemfield	29°53', 150°28'	Central, NSW	sub-volcanic leads	6
Cudgegong River	32°50', 149°50'	Dubbo, NSW	sub-volcanic leads	6
Oberon	33°45', 149°50'	Abercrombie, NSW	very rare	7
Crookwell	34°30', 149°30'	Abercrombie, NSW	rare finds extend to Graben Gullen	1
Tumbarumba	35°45', 148°00'	Snowy, NSW	common	1
Upper Yarra	37°40', 145°52'	Nerrim, Vic		8
Tubba Rubba Ck	38°14', 145°05'	Flinders, Vic	restricted alluvial distribution	8
Kernot, Bass River	38°23', 145°37'	Flinders, Vic	common mauve grains	9
Blue Ck, Trentham	37°25', 144°18'	Woodend, Vic	rare, in sub-volcanic lead	9
Weld River	41°10', 147°53'	NE Tasmania	rare, shattered small grains	10

References: 1. MacNevin and Holmes (1980); 2. Sutherland *et al.* (1993a); 3. A.D. Robertson, Queensland Department of Mineral and Energy, pers.comm. (1995); 4. Coldham (1985); 5. Authors' data; 6. MacNevin (1977); 7. M. Walburn, pers.comm. (1995); 8. Museum of Victoria collections, W. D. Birch, pers.comm. (1988); 9. J.D. Hollis, pers.comm. (1995); 9. W.L. Matthews, Tasmanian Department of Mines, pers.comm. (1990). Volcanic provinces after Johnson (1989).

side (Fig.1, modified from Sutherland *et al.*, 1993a). The area is rugged and covered by soils and vegetation in many parts. Rubies are found up to 1420 m a.s.l., that is relatively high in the volcanic sequence, which extends from 850 m to 1545 m a.s.l. Around Gloucester Tops, single ruby grains weigh up to 3 carats and provide cut stones up to 1 carat, while single sapphires weigh up to 5.5 carats and provide cut stones up to 1.5 carats weight (A.W. Chubb, pers.comm., 1970). The ruby-bearing aggregates came from 1260–1340 m a.s.l. at the heads of drainages dissecting basalt remnants on the interfluvium between the Kerripit and Gloucester Rivers near Mt McKenzie on Gloucester Tops (Fig.1).

The Barrington basalts overlie folded Palaeozoic beds intruded by a late Permian granodiorite pluton (265–281 Ma; Collins *et al.*, 1993; Kimbrough *et al.*, 1993). The basalts are thickest over magnetic and gravity anomalies associated with a large subvolcanic magma chamber at 4 to 13 km depth (Wellman, 1989). The province consists of largely unevolved tholeiitic basalts, alkali basalts, basanites and intercalated alluvial leads and lacustrine deposits (Mason, 1982; Pain, 1983). The main shield was built from 60–54 Ma ago, but later eruptive episodes date to at least 27 Ma ago, based on K-Ar basalt and zircon fission track dating (Wellman and McDougall, 1974; Pain, 1983; Sutherland *et al.*, 1993a and

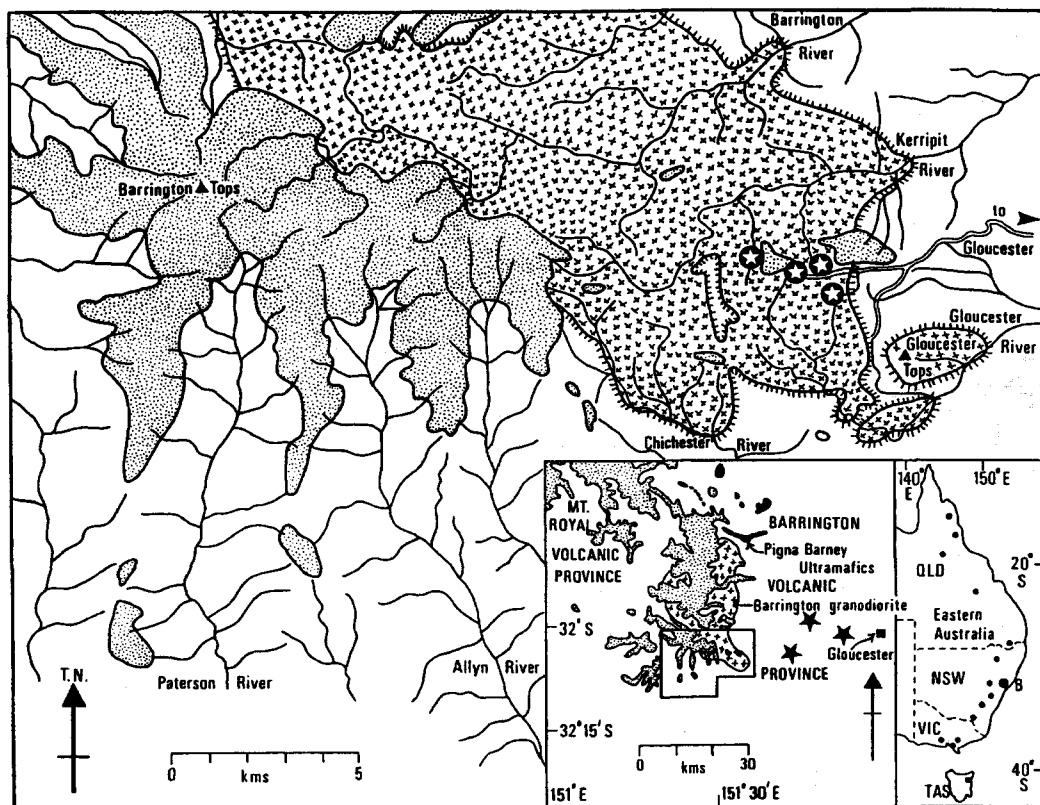


FIG. 1. Geological Map of Barrington Tops-Gloucester Tops region, New South Wales, simplified from the Camberwell and Dungog 1:100 000 Geological Sheets (1991). The map shows the distribution of present drainage (thin lines) in relation to Tertiary basalt (stippled areas) of the Barrington Volcanic Province and Permian Barrington Tops Granodiorite intrusion (crosses) and the sites which yielded unusual coloured sapphires and miniature ruby-sapphire-sapphirine-spinel aggregates (circled stars). The Granodiorite intrusive contacts against the Palaeozoic beds (clear areas) are marked as hatched lines. A large inset shows the detailed area in relation to the surrounding Tertiary volcanic provinces, Jurassic alnöitic intrusives (stars), Permian granodiorite and Palaeozoic ultramafic bodies (solid black areas). A small inset shows the location of the Barrington ruby field (larger dot) and other ruby sites (smaller dots) in eastern Australia as listed in Table 1.

unpublished data). Ultramafic lamprophyre breccia pipes and alnöite bodies of Jurassic age intrude the Palaeozoic beds and carry high pressure xenoliths and xenocrysts (MacNevin, 1977; Sutherland, 1985; O'Reilly *et al.*, 1988; Rock, 1991).

Mineral suites

The corroded and reacted corundum-bearing aggregates range from 1 to 4 mm across (Fig. 2). Ten were selected for photography and preliminary investigation by scanning electron microscope. Minerals in the aggregates (Table 2) include corundum (ruby and sapphire), sapphirine and spinel (pleonaste and

chromian pleonaste). Sapphires include colourless, yellow, orange, green, blue and pink grains, sapphirine ranges from white through blue to dark green, to near opaque grains and spinels form opaque grains. All these minerals and varieties can occur in a single aggregate, as largely anhedral intergrowths with sharp contacts. The sapphirine and corundum may show a reaction rim of pleonaste spinel (Fig. 3), which has been abraded away to different degrees in the alluvial environment.

Minerals identified in the heavy mineral concentrates that contain the aggregates include corundum, zircon, ilmenite, spinel, magnetite, olivine, diopside, enstatite and pyrite. Corundum ranges from colour-

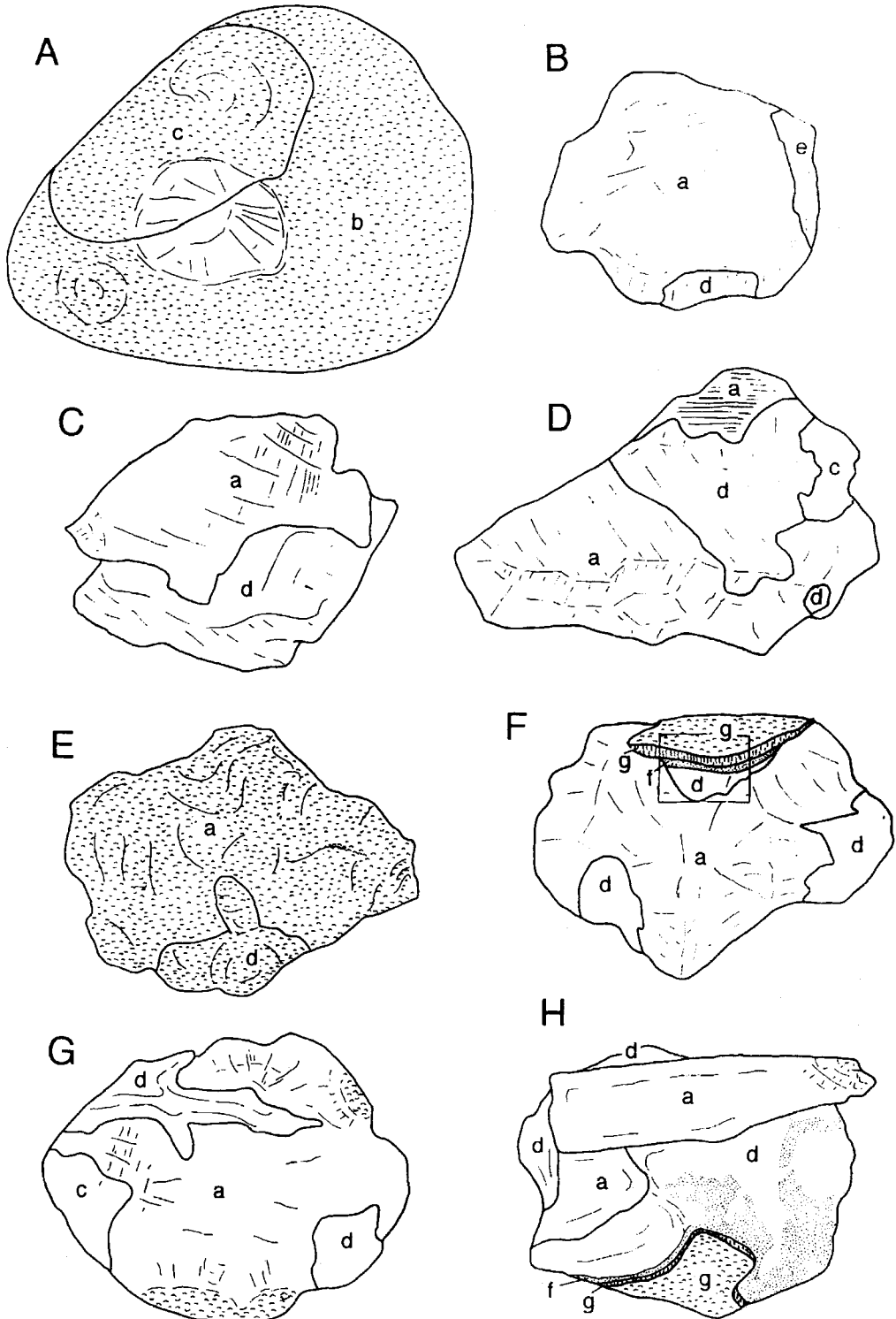


TABLE 2. Analysed aggregate assemblages, Gloucester Tops

Ruby—white to dark green sapphirine ($\text{Mg}_{89-90}\text{Fe}_{10-11}$), spinel reaction rim ($\text{Mg}_{68-70}\text{Fe}_{30-32}$)
Ruby—green sapphirine ($\text{Mg}_{90}\text{Fe}_{10}$), white to black spinel reaction rim ($\text{Mg}_{60}\text{Fe}_{40}$)
Ruby—black chromian spinel ($\text{Mg}_{58}\text{Fe}_{28}\text{Cr}_{14}$)
Ruby—black spinel ($\text{Mg}_{68-70}\text{Fe}_{30-32}$)
Pink sapphire—orange sapphire—green to blue sapphirine ($\text{Mg}_{90}\text{Fe}_{10}$)
Pink sapphire—black spinel ($\text{Mg}_{76-77}\text{Fe}_{23-24}$)—cordierite ? ($\text{Mg}_{29-50}\text{Fe}_{50-71}$).
Pink sapphire—white sapphire—dark green spinel ($\text{Mg}_{63-67}\text{Fe}_{32-38}$)
Pink sapphire—black spinel ($\text{Mg}_{66-75}\text{Fe}_{25-34}$)
White sapphire—black spinel ($\text{Mg}_{62-68}\text{Fe}_{32-38}$)

less transparent to black opaque material. Sapphire colours include colourless, yellow, orange, green, blue and mauve, with rare parti-coloured and colour change sapphires (pale grey blue to pale green blue in daylight, pale pink to pink in incandescent light). Pale to medium pink sapphires (up to 0.5 wt.% Cr_2O_3) grade into purple red and dark red rubies (with strong Cr and Fe absorption lines and up to 1.4 wt.% Cr_2O_3 ; Sutherland *et al.* 1993a). Two suites of sapphires appear to be present. One suite shows strong colour zoning in hexagonal bands in green, blue, white or brown. Many of these exhibit etched or broken barrel habits, carry inclusions of silk (fine rutile needles and oriented laths of rutile, hematite or iron-titanium oxide along crystallographic directions) and in some cases form asterated (star) stones. These features are typical of many east Australian sapphires (Coldham, 1985). The other more unusual suite includes magmatically rounded, heavily etched, pastel coloured yellow, blue, green, orange and mauve sapphires, and also includes pink to red

corundums. Some stones exhibit strong dichroism or, more rarely, colour change. They lack distinct crystal forms, strong crystallographic colour banding or silk inclusions, and are typical of the sapphires and rubies found in the corundum-sapphirine-spinel aggregates. Rubies in this suite contain chromian pleonaste as dominant inclusions (up to 0.1–12 wt.% Cr_2O_3 ; Sutherland *et al.*, 1993b).

Zircon ranges from white through yellow, pink, brown and red, and includes abraded, corroded crystals as well as unabraded euhedral crystals. They give fission track ages of 27–55 Ma. A distinctive cream to honey yellow coloured, euhedral zircon is enriched in uranium (1028–1488 ppm U for 9 analyses), compared to the older zircon types from the Barrington shield (av. 33–520 ppm U for 22 analyses). This zircon yields significantly younger fission track age of 4–5 Ma (Australian Museum unpublished reports) and suggests possible eruption of the corundum-bearing aggregates during a much later stage of Barrington volcanic activity.

FIG. 2. Sketches of corundum-rich aggregates illustrating combinations of intergrown ruby (a), blue sapphire (b), colourless to pale yellow sapphire (c), sapphirine (d) and spinel (e), with some showing melt reaction skins of spinel (f and g). Corroded surfaces are shown as hummocky stipple and fractured surfaces as clear areas, marked with fracture lines and edges. The largest aggregate A is 4 mm across. The remainder are drawn to scale. A. blue-violet sapphire (b) and pale yellow sapphire (c); rounded aggregate with glossy resorbed surface showing corroded embayments, probably crystal sockets – a circular conchoidal fracture cuts across the grain boundary. B. Pale pink, opaque corundum (a), black sapphirine (d) and black spinel (e); angular aggregate with fresh fractured surfaces. C. Ruby (a) and dark green-blue sapphirine (d); sharp edged angular aggregate with conchoidally fractured curved surfaces. D. Pale pink transparent ruby (a), part displaying distinct twinning, transparent colourless sapphire (c), green-blue sapphirine (d); angular aggregate with fresh fractured surfaces. E. Pale pink, transparent ruby (a), and dark green-blue sapphirine (d); rounded aggregate displaying a polished, corroded and embayed surface. F. Pink-orange ruby (a) and dark green-blue sapphirine (d); aggregate with fractured surfaces and a small area of original reaction surface of white granular spinel (f) on sapphirine and black spinel (g) on white spinel and ruby. G. Red transparent ruby (a), colourless transparent sapphire (c) and green-blue sapphirine (d); angular fractured surfaces with areas of original polished surface. H. Pink ruby (a) and blue-green sapphirine (d); fracture surfaces and an area of original reaction surface of black spinel (g); undamaged sapphirine surface with reaction surface chipped away shows patches of glassy white sapphirine (dotted), passing into white spinel (f). Reflected light photograph (Fig. 3) was taken within the rectangle marked in aggregate F after it was polished.

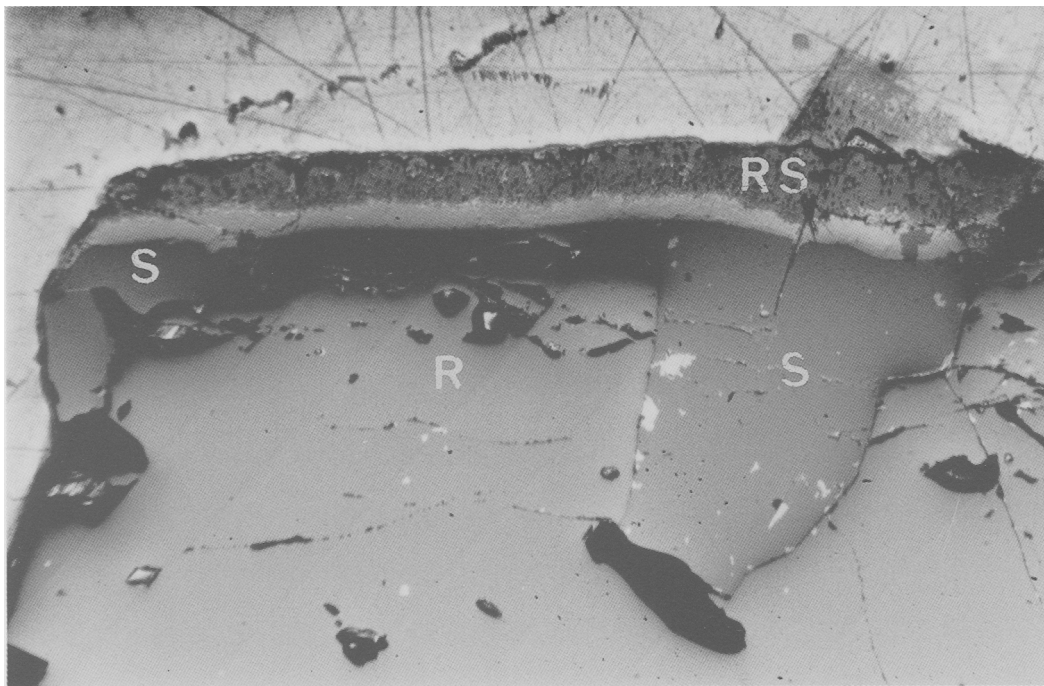


FIG. 3. Photomicrograph of ruby (basal crystal showing inclined twinning; R) intergrown with sapphirine (central crystal; S), which shows a reaction rim of spinel (upper banded light to grey microgranular material; RS). Base of photo is approximately 1 mm across. The top part of photo consists of polished section mounting material.

Analytical methods

Trace cations in corundums in the aggregates were investigated by EDS microanalysis (Philips SEM505 scanning electron microscope; Electron Microscope Unit, University of Sydney) to detect colouring cation values above background levels. Compositions of sapphirines and spinels in nine corundum aggregates were quantitatively analysed using an automated Cameca SX50 CAMEBAX electron micro-probe, equipped with four WDS spectrometers and EDS attachment, in the Material Sciences Faculty, University of New South Wales (Table 3). The operating conditions included an accelerating voltage of 15 kV, a sample current of 20 nA, PAPS software for processing raw counts and a ASTIMEX standard block. Elements analysed for and standards used to determine their oxide equivalents were Si (diopside), Ti (rutile), Al (sanidine), Cr (chromite), Fe (hematite), Mn (rhodonite), Mg (diopside), Ca (diopside), Na (albite), K (sanidine) and Ni (nickel metal).

In addition, opaque oxide inclusions in a blue sapphire crystal from Barrington, typical of the more usual Australian sapphires, were also analysed for

comparison with the aggregate pleonastes and with inclusions in sapphires from New England gem fields in New South Wales (Table 4).

Results

Colourless to pale yellow sapphires in the aggregates lacked significant trace cations. Yellow to green sapphires contained Fe, blue sapphires Fe and Ti and orange sapphires Ti and Fe, while pink to red corundums showed increasing Fe and Cr, sometimes with Ti and Mg, with depth of colour. The ranges and compositions of sapphirine, pleonaste, chromian pleonaste and the reaction rim spinel are summarized in Tables 2 and 3. The sapphirines are Mg-rich (Mg_{87-90} , Fe_{10-13}). Cation proportions, based on 20 oxygens, were recalculated to 14 by allocation of total Fe after the method of Droop (1987). The cation proportions are used to plot oxide molecular sums on the $\text{MgO} + \text{FeO}$, $\text{Al}_2\text{O}_3 + \text{Fe}_2\text{O}_3$, SiO_2 composition diagram. The mol. % oxide sums $\text{MgO} + \text{FeO} = 36.8-37.5$, $\text{Al}_2\text{O}_3 + \text{Fe}_2\text{O}_3 = 44.9-47.2$, $\text{SiO}_2 = 16.0-17.0$ plot close to the theoretical $(\text{Mg}, \text{Fe}^{2+}) \text{Si} \rightleftharpoons (\text{Fe}^{3+})$ substitution line and near a 7:9:3 sapphirine composition (Fig. 4).

TABLE 3. Representative sapphirine and spinel analyses, Gloucester Tops aggregates, NSW

Oxide wt. %	Sapphirine		Pleonaste		Cr-Pleonaste		Reaction	Spinel
	range	av.	range	av.	range	av.	range	av.
SiO ₂	13.00–13.94	13.53	0.00–0.05	0.02	0.00–0.04	0.02	0.01–0.05	0.03
TiO ₂	0.00–0.05	0.02	0.00–0.36	0.07	0.02–0.08	0.04	0.29–0.48	0.36
Al ₂ O ₃	61.98–64.15	62.68	62.75–67.21	66.09	57.69–65.18	63.07	61.90–62.58	62.27
Cr ₂ O ₃	0.16–0.60	0.40	0.04–0.38	0.18	1.05–8.51	3.05	0.58–0.64	0.62
FeO*	3.64–5.24	4.01	11.59–17.89	13.85	14.65–15.84	15.12	15.27–19.95	17.25
MnO	0.00–0.11	0.01	0.06–0.22	0.11	0.01–0.11	0.05	0.16–0.19	0.18
MgO	18.91–19.40	19.14	16.06–21.25	19.10	16.64–18.08	17.61	16.62–19.65	18.56
CaO	0.00–0.11	0.07	0.00–0.02	0.01	0.00–0.02	0.01	0.00–0.03	0.02
Na ₂ O	0.00–0.06	0.02	0.00–0.02	0.01	0.01–0.04	0.02	0.00–0.01	0.00
K ₂ O	0.00–0.03	0.01	0.00–0.02	0.01	0.00–0.01	0.00	0.00–0.01	0.00
NiO	0.11–0.32	0.24	0.04–0.27	0.17	0.09–0.33	0.20	0.16–0.32	0.23
Total	99.60–100.73	100.13	98.90–100.82	99.62	98.80–99.44	99.19	98.90–100.35	99.52
	(9 analyses)		(11 analyses)		(4 analyses)		(3 analyses)	
	Mg _{87–90} Fe _{10–13}		Mg _{62–77} Fe _{23–28}		Mg _{58–67} Fe _{28–34} Cr _{2–14}		Mg _{60–70} Fe _{30–40}	

FeO* = Total iron as FeO. Analysts C. Nockolds and R.R. Coenraads

Spinel compositions (Mg_{62–77} Fe_{23–38}) mainly fall in the pleonaste range with an average end member composition of Sp 72.6, Hc 26.7, Mt 0.3, Cm 0.2, Usp 0.1%, with some grains (Mg_{58–67} Fe_{28–34} Cr_{2–14}) falling in the chromian pleonaste range with an average composition of Sp 68.4, Hc 28.5, Cm 3.1, Usp 0.1%. Reaction rim spinel formed on sapphirine is on average more Fe-enriched

TABLE 4. Representative Fe-rich spinel analyses, inclusions in blue sapphire, NSW

Oxide wt. %	Hercynite 1		Hercynite 2	Hercynite ⁺
	range	av.		range
SiO ₂	0.05–0.06	0.05	0.02	0.00–0.09
TiO ₂	1.66–2.10	1.88	0.91	0.13–1.05
Al ₂ O ₃	25.73–27.20	26.47	38.58	47.76–58.11
Cr ₂ O ₃	0.00–0.01	0.01	0.00	0.00
Fe ₂ O ₃ *	33.65–34.43	34.04	20.75	
FeO	34.37–34.42	34.40	35.72	30.39–55.57
MnO	0.12–0.15	0.14	0.07	0.49–0.85
MgO	1.45–1.58	1.52	1.28	0.08–6.09
NiO	0.00–0.03	0.02	0.09	
Total	98.42–98.54	98.48	97.42	
Analyses	2		1	7
Hc	51.4–54.0	52.7	73.1	
Mt	34.7–35.3	35.0	18.5	
Mf	7.3–8.0	7.7	6.1	
Usp	4.1–5.4	4.8	2.2	

Hercynite 1 and 2, Barrington Volcanic Province

⁺ New England Central Volcanic Province (Coenraads, 1992)

* Recalculated from Total FeO, following Droop (1987)

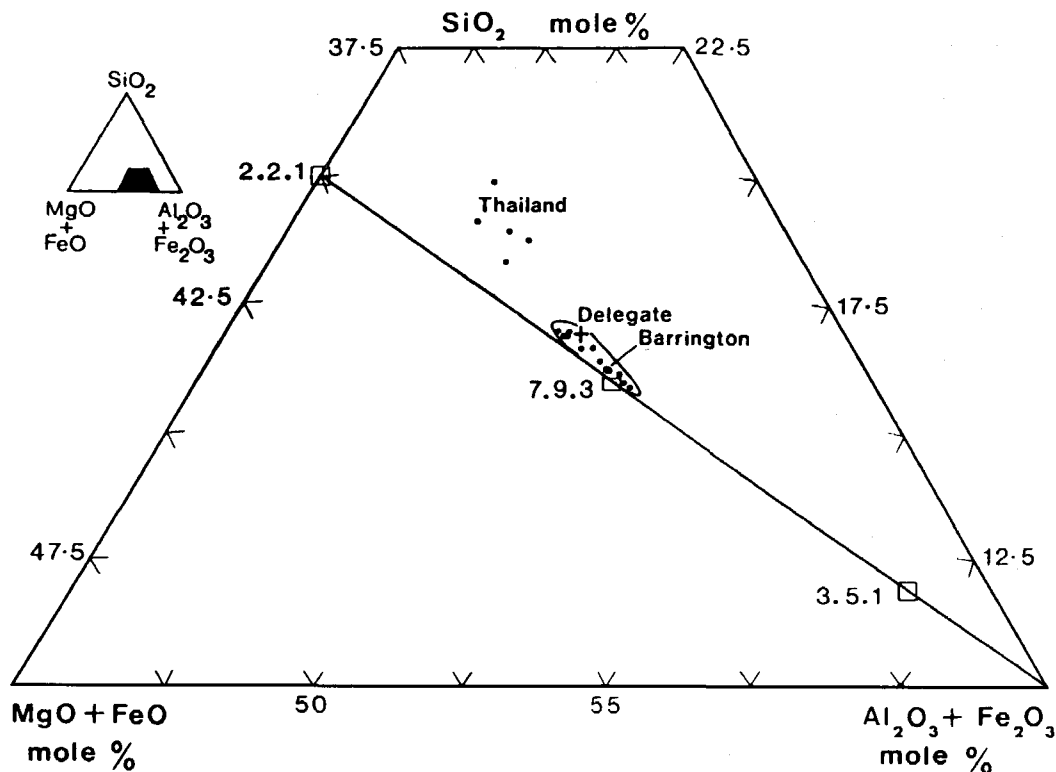


FIG. 4. Relevant portion of $\text{MgO} + \text{FeO}.\text{Al}_2\text{O}_3 + \text{Fe}_2\text{O}_3.\text{SiO}_2$ mole % triangular diagram showing plots of sapphirine compositions from corundum-bearing aggregates, with theoretical compositional members shown as designated squares (after Deer *et al.*, 1978, p. 622). Barrington sapphirine plots (dots) are recalculated for stoichiometric Fe^{3+} and enclosed in a field. Thailand (Rubywell Mine) sapphirine analyses have no Fe^{3+} for reallocation and their plots are not constrained in a field (R.R. Coenraads, analyses). The cross represents the plot of sapphirine in a granulite xenolith from the Delegate breccia pipe (Griffin and O'Reilly, 1986). The extent of the detailed diagram in the full compositional triangle is shown in a small inset.

($\text{Mg}_{60-70}\text{Fe}_{30-40}$) and is pleonaste with an average end member composition of Sp 71.8, Hc 23.4, Mt 3.5, Usp 0.7, Cm 0.6%. The high Mg/Fe ratio of the reaction rim spinel reflects the high Mg/Fe of the sapphirine, but may also reflect a high Mg/Fe of the host melt as this spinel also develops on corundum.

In contrast, the oxide inclusions in the blue sapphire, more typical of eastern Australian suites, are far more Fe-rich ($\text{Fe}_{96}, \text{Mg}_4$; Table 4) and belong to the hercynite-magnetite series with an end member composition range of Hc 51.4–73.1, Mt 18.5–35.3, Mf 6.1–8.0, Usp 2.2–5.4%. Experimental work on miscibility in the system $\text{FeO}-\text{Fe}_2\text{O}_3-\text{Fe}_2\text{Al}_2\text{O}_4$ (Lindsley, 1976, p. L-80, Fig. L-29) indicates these compositions are compatible with crystallization temperatures over 800–850°C.

One aggregate (white sapphire-spinel) contains a few small dark grains (<0.05 mm) which would not take a high polish. These yield low oxide totals (80–87 wt.%), probably due to the irregular texture, but indicate the mineral is an Fe, Mg aluminium silicate. Recalculations of oxides to 100 wt.% gives SiO_2 47–50, Al_2O_3 33–37, total FeO 10–13 and MgO 3–6 wt.% and these oxide totals suggest that the mineral is cordierite.

Origin of ruby-sapphire-sapphirine-spinel aggregates

The corrosive etching of corundum and the spinel reaction rims on sapphirine and corundum suggest magmatic transport, presumably in basalt eruptives of

the Barrington volcano. The aggregates probably represent miniature xenoliths and the accompanying ruby and sapphire grains probably represent disaggregated xenocrysts eroded out of basalts. Distance travelled by the aggregates in the alluvial system since their release from the host rock has been minimal as suggested by; the preservation of the aggregates themselves, reaction rims on the surfaces of the aggregates and individual crystals, as well as the presence of sharp edged, unworn euhedra among accompanying zircons. The origin of the coarse grained rocks of which the aggregates were part before their magmatic incorporation is more problematical, but the co-existence of corundum, sapphirine and spinel provides some constraints on their origin in the context of the surrounding geological setting.

Gem rubies and sapphires are produced from both metamorphic and igneous terrains (Keller, 1990; Hughes, 1990) and can arise from metasomatic desilicification reactions associated with pegmatitic intrusion in serpentinized ultramafic bodies (Keller, 1992). Sapphirine is usually found in metamorphic assemblages, but also crystallizes in igneous systems (Deer *et al.*, 1978). It can be found with corundum, but is also often associated with other mineral phases not observed in the Barrington Tops aggregates (e.g. pyroxenes, feldspars, garnets, micas, amphiboles, sillimanite). Sapphirine is a rare product in contact metamorphism, generally in xenoliths recrystallized by high temperature mafic liquids. Sapphirine-pleonaste ($\text{Mg}_{55}\text{Fe}_{45}$)-corundum assemblages were described from metasomatized hornfels, where peridotitic magma interacted with country rock schists in the Cortlandt mafic complex, New York (Barker, 1964). However, these do not match the gemmy Gloucester Tops aggregates, being finer grained and associated with ubiquitous magnetite and ilmeno-hematite and minor biotite and plagioclase. Sapphirine-spinel-corundum-rutile parageneses enclosed in feldspathic haloes were analysed from metapelitic xenoliths in lamprophyre dykes at Pope Harbour, Nova Scotia, Canada (Owen and Greenough, 1991). These were interpreted as refractory residues formed by incongruent melting of biotite and other phases and differ from the Barrington aggregates in much finer grain size and very subordinate presence of corundum. A sapphire-pink corundum xenolith (?) is known from granite, but this shows euhedral crystals (Mountain, 1939). Thus, ruby-sapphire-sapphirine-spinel assemblages, such as observed at Barrington Tops, do not seem documented in the literature. A sapphirine inclusion in ruby from a Thai basalt field is described by Koivula and Fryer (1987).

Several possibilities exist for formation of the aggregates in terms of the geology of the

Barrington area, assuming the mineral assemblage represents complete rather than refractory residues. The paucity of different mineral inclusions in the aggregate minerals tends to support an intact assemblage and, together with the straight edged mineral grain boundaries, implies that it is at, or near, equilibrium.

Contact metamorphism of Palaeozoic beds by the Permian Barrington granodiorite (Fig. 1) reaches elevations higher than the corundum occurrences at Gloucester Tops, but the effects are largely restricted to minor cherty hornfels formation. Other coarser effects could be more extensive at depth, or occur within xenolithic pods. Another possibility is metasomatism by magmatic infiltrations into Cr-bearing sources, such as serpentinized ultramafic bodies, similar to the Pigna Barney ophiolite northeast of Barrington Tops (Kimbrough *et al.* 1993). No ultramafic body is exposed further south around Barrington and Gloucester Tops, but could be present as an extension along a fault at depth. High-temperature recrystallization or metasomatism of aluminous material incorporated into mafic bodies below Gloucester Tops, involving either the Cainozoic basaltic magma chambers or Jurassic alnoitic pipes (Fig. 1), represent further possibilities. High pressure recrystallization of aluminous material, introduced below continental areas during oceanic subduction, has been recently proposed for gem corundum formation (Levinson and Cook, 1995). Older, subducted island arc and altered seafloor basalt most likely exists below the Gloucester area based on isotopic signatures in granulite xenoliths in Jurassic breccia pipes (O'Reilly *et al.*, 1988) and on evidence that the Barrington granodiorite was probably generated from oceanic mantle (Kimbrough *et al.*, 1993).

Crystallizations from melts represent further alternatives for the formation of the mineral assemblage. These could include Al-rich anatectic melts produced by intrusion of the Barrington granodiorite pluton or Barrington Tops basalt chamber into the lithosphere. The Barrington granodiorite is an unusual, high temperature, primitive suite (Eggins and Hensen, 1987), while relatively unevolved high temperature basalts dominate the Tertiary Barrington shield (Mason, 1989; F.L. Sutherland, unpublished data) and sporadic strongly undersaturated Jurassic intrusives carry high pressure xenoliths and xenocrysts (O'Reilly *et al.*, 1988; Rock, 1991). Crystallization from the Jurassic-Tertiary mafic magmas at high pressures and temperatures, forming liquidus or near liquidus aggregates could possibly produce sapphirine-bearing assemblages, as proposed within the anorthosite-forsterite-quartz system (Fig. 5b; Liu and Presnall, 1990).

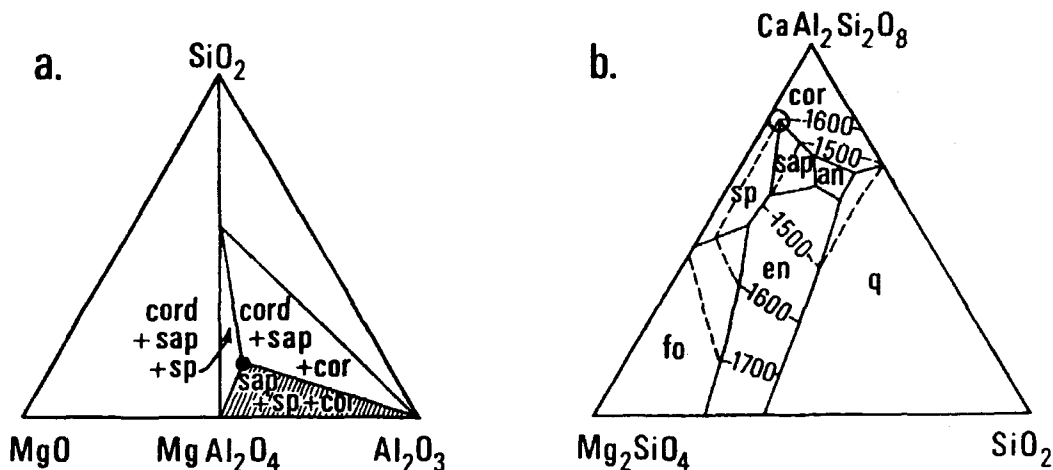


FIG. 5. (a) Al_2O_3 - MgO - SiO_2 triangular diagram showing compositional field in which corundum (cor) + spinel (sp) + sapphire (sap) can co-exist below 1460°C at one atmosphere (shaded area). The point $\text{Mg}_4\text{Al}_8\text{Si}_2\text{O}_{20}$ (solid dot) is where these phases can also co-exist with cordierite (cord) in the cord + sap + sp and cord + sap + cor fields below 1386°C . Simplified from Smart and Glasser (1976). (b) $\text{CaAl}_2\text{Si}_2\text{O}_8$ - Mg_2SiO_4 - SiO_2 phase diagram at 20 kbar showing liquidus temperatures (dashed lines) in relation to the mineral phases boundaries (solid lines) for corundum (cor), spinel (sp), sapphire (sap), anorthite (an), forsterite (fo), enstatite (en) and quartz (q). The point where cor, sp and sap coexist at 1575°C is circled. Simplified from Liu and Presnall (1990).

To guide assignment of the aluminous corundum-sapphire aggregates, some phase relationships at different temperatures (T) and pressures (P) are considered. In the MgO - Al_2O_3 - SiO_2 system at one atmosphere, sapphire, spinel and corundum co-exist in the compositional field MgAl_2O_4 - $\text{Mg}_4\text{Al}_8\text{Si}_2\text{O}_{20}$ - Al_2O_3 (together with cordierite at $\text{Mg}_4\text{Al}_8\text{Si}_2\text{O}_{20}$), but only at temperatures below 1460°C Fig. 5a (Smart and Glasser, 1976). Addition of Na_2O , CaO and Fe_2O_3 (in individual amounts up to 1.5 wt.%) makes little difference to reactions in the system between 1360 – 1410°C . Above $\sim 1460^\circ\text{C}$, the corundum and sapphire fields remain separate, even at 15 kbar (Taylor, 1973). More siliceous material however, with a pelitic composition containing up to 8 wt.% FeO , when subjected to various PT and H_2O and CO_2 conditions, did not produce coexisting corundum-sapphire-spinel (Bertrand *et al.*, 1991). Hence, the Gloucester Tops assemblages could represent recrystallization of aluminous materials with <20 wt.% SiO_2 and <50 wt.% MgO at temperatures up to 1460°C (Fig. 5a).

The CaO - MgO - Al_2O_3 - SiO_2 system is more relevant to basaltic liquids and phase relationships from 1–20 kbar are compared in Liu and Presnall (1990). A primary sapphire field appears between 10–20 kbar (Fig. 5b) and a liquidus piercing point for a corundum-sapphire-spinel assemblage is located at

1575°C for a composition of $\text{An}_{81}\text{Fo}_{17}\text{Q}_2$ wt.%. Thus, Gloucester Tops aggregates could represent potential crystallization from high T anatectic melts of sources rich in calcic feldspathic material or possibly from high PT fractionation of basaltic magma (Fig. 5b). The relatively high Ca, Al silicate content and low degree of SiO_2 saturation necessary for the potential basaltic parent (Fig. 5b), and participation of Cr in the aggregate phases (ruby and chromian spinel) would suggest high P crystallization related to either of the two typical undersaturated parental magmas represented in the Barrington area–Jurassic alnoite and Tertiary basanite (Table 5).

The appearance of corundum in high PT experiments on Mauritius basanite (Fiske and Ford, 1984) deserves some consideration as both the Barrington and Mauritius volcanoes erupted similar primary basanites (Table 5). The corundum was found in an experimental run at 1500°C and 30 kbar in heterogeneous glass, which ranged from the starting basanite composition to Al_2O_3 enriched compositions similar to that observed in glass surrounding ultramafic xenoliths in the basanite (Table 5). The Cr, Fe and Si analysed in the experimental corundum suggests that the grains were not fragments of alumina from the furnace assembly and one analysed corundum was a euhedral grain (M.R. Fiske, pers. comm., 1992). Aluminous glasses found within the ultramafic xenoliths and in the host groundmass

TABLE 5. Representative alkaline rock compositions, Barrington and Mauritius

Analysis (wt.%)	1	2	3	4	5
SiO ₂	36.2	41.4	42.8	55.2	63.2
TiO ₂	3.3	1.9	2.7	1.1	0.7
Al ₂ O ₃	11.2	13.3	12.1	23.9	15.7
Fe ₂ O ₃	1.8	2.4	2.7	0.8	0.4
FeO	8.9	8.6	9.8	2.9	1.3
MnO	0.2	0.2	0.2	0.1	0.0
MgO	10.3	12.3	12.6	0.8	1.9
CaO	13.0	12.6	11.1	1.0	0.4
Na ₂ O	2.2	3.5	2.6	9.2	4.7
K ₂ O	2.4	0.9	1.3	4.9	5.9
P ₂ O ₅	1.1	1.3	0.5	0.2	0.0
CO ₂	4.2			—	
H ₂ O+	5.1	1.4	1.6+	0.0+	5.9+
Total	99.9	99.8	100.0	100.1	100.1

Fe₂O₃/FeO ratio set at 0.2, + H₂O by difference.

CIPW Nom	1	2	3	4	5
Q					9.6
Or	15.1	5.1	8.0	29.0	37.1
Ab	3.7	0.3	4.5	34.9	42.4
An	14.5	18.4	17.8	3.2	2.1
Ne	8.5	15.8	9.7	23.3	
Di	14.9	29.2	28.0		
Hy					6.0
Ol	20.5	20.2	21.8	3.7	
Mt	3.5	3.5	4.0	1.2	0.6
Il	6.6	3.7	5.2	2.1	1.4
Ap	2.6	3.0	1.2	0.6	
CC	10.0				
C				2.3	0.9
Mg N°.	69.0	71.7	69.7	32.3	72.0
Differentiation Index	27.3	21.2	22.2	87.1	89.1

1. Alnöite, Cobark River, Barrington, XRF analysis, University of Sydney; L.R. Raynor.
2. Basanite, Thunderbolt Lookout, Barrington, ICP analysis, Amdel Laboratories, Adelaide.
3. Basanite, Mauritius, from Fiske and Forde (1984).
4. Glass 1, in basanite/ultramafic xenolith, Mauritius, from Fiske and Ford (1984).
5. Glass 3, in basanite/ultramafic xenolith, Mauritius, from Fiske and Ford (1984).

around the xenoliths in the Mauritius basanite most probably incorporated melt products of Al-rich phases. The glasses range from nepheline to quartz-normative compositions and, importantly, are corundum-normative (Table 5).

Thus, initial melting of ultramafic rocks by basanite magmas invading them at high *PT*, may provide small volume anatectic melts capable of crystallizing co-existing aluminous minerals. Melting

of accessory Cr-bearing phases in the ultramafic rocks (eg. chromian spinel or chromite) would contribute irregular concentrations of Cr allowing both ruby and sapphire to crystallize together as millimetre-sized grains. The Barrington primary basanite (Table 5, analysis 2) contains sparse coarse to medium sized olivine xenocrysts. These include olivine (Mg₉₁Fe₉) containing subhedral chromite inclusions (Cr₅₂Mg₂₄Fe₂₄) and olivine (Mg₈₆)

containing subhedral chromian pleonaste inclusions ($\text{Mg}_{68}\text{Fe}_{26}\text{Cr}_6$) and suggest Cr-bearing, olivine-rich bodies exist under the central part of the Barrington shield volcano. The above olivines are not typical of normal spinel ilmenite mantle in eastern Australia, but could come from abnormal, metasomatized mantle, or ultramafic cumulates.

Discussion

An unequivocal origin for the Barrington aggregates is difficult to assign on present data. The largely anhedral intergrowth of the co-existing phases in mm-sized aggregates does not strongly specify igneous or metamorphic crystallization, as accumulative textures can resemble metamorphic granulite textures (Vernon, 1970) and are not always diagnostic of strict igneous origin (McBirney and Hunter, 1995). Sapphirine is commonly thought to be metamorphic, but igneous sapphirine is reported (Deer *et al.*, 1978). Al-rich sapphirines were considered low pressure types and Si-rich sapphirines high pressure types based on early studies of sapphirine (Taylor, 1973; Bishop and Newton, 1975). However, later studies showed that sapphirine compositions depended on bulk rock compositions, as well as *PT* conditions (Griffin and O'Reilly, 1986). The Barrington 7:9:3 sapphirine composition overlaps that of high pressure sapphirine in a garnet granulite xenolith from the Delegate pipe in eastern Australia (Griffin and O'Reilly, 1986; Fig. 4) and illustrates the problem of correlating natural sapphirine compositions with *PT* conditions.

An empirical sapphirine-spinel thermometer was developed to investigate sapphirine-spinel-corundum-rutile assemblages in xenoliths in Nova Scotia lamprophyres (Owen and Greenough, 1991). This Mg-Fe exchange thermometer can be applied to the Barrington aggregates. The thermometer shows a moderate increase in temperature dependence with partitioning coefficient *Kd* for Mg and Fe in the sapphirine-spinel pair. This is summarised in the expression $T(^{\circ}\text{C}) = [800 + (228 \ln Kd)] - 273$ where $Kd = (X_{\text{SpFe}}/X_{\text{SpMg}})/(X_{\text{SaFe}}/X_{\text{SaMg}})$. Using the average sapphirine and spinel compositions and adjacent sapphirine-spinel pair analyses, the thermometer gives temperatures ranging from 780–940°C. An estimate for sapphirine and an outermost reaction rim spinel gave 1015°C. The analysed Barrington sapphirines used in the calculations are appreciably lower in Fe ($\text{Fe}^{2+}/\text{Mg} + \text{Fe}^{2+}$ 0.05–0.8), but more oxidised in Fe ($\text{Fe}^{3+}/\text{Fe}^{2+} + \text{Fe}^{3+}$, 0.41–0.47) than the Nova Scotia xenoliths (X_{Fe} 0.18–0.26, $X_{\text{Fe}^{3+}}$ 0.03–0.15; Owen and Greenough, 1991). Thus, the precision of the Barrington results are probably less than $\pm 100^{\circ}\text{C}$ as the applicability of the thermometer

to more oxidized and high temperature sapphirine assemblages is less certain. However, the results suggest moderately high temperatures of formation for the Barrington assemblages and subsequent reaction in a magmatic host at $>1000^{\circ}\text{C}$. The assemblage temperatures are below those expected for liquidus precipitates from mafic-ultramafic magmas, but would not preclude reequilibration of original high-*T* cumulates under later cooler conditions. The temperatures are compatible with crystallization from anatectic felsic melts, metamorphic/metasomatic contact reactions or deep seated metamorphism. The crystallization of Mg-rich, Fe^{3+} -bearing sapphirine, as in the Barrington aggregates, is usually favoured under conditions of elevated oxygen fugacity (Hensen, 1986).

Although a precise origin for the Barrington aggregates remains uncertain, the discovery of these co-existing aluminous mineral phases is a breakthrough in further understanding of ruby occurrences in gemfields associated with basaltic volcanic provinces. The main sources of such ruby come from southeast Asia (Keller, 1990; Vichit, 1992), extending from eastern Thailand, from the Chanthaburi-Trat province (characterized by rubies, blue and green sapphires) through Trat (rubies) into western Kampuchea and the Battambang (Pailin) province (rubies and sapphires). Thai and Kampuchean rubies share similar characteristics, generally lacking distinct crystal form, colour zoning or significant development of rutile silk inclusions, and carry a common set of inclusions (Gübelin and Koivula, 1986; Hughes, 1990). Inclusions present are boehmite, pyrrhotite commonly altered to goethite, almandine or pyrope garnet, apatite, plagioclase, olivine, diopside and negative crystals, and are often surrounded by liquid fingerprints or feathers giving the so called 'saturn' inclusions (Hughes, 1990, pp. 81–83). Locally, rubies may lack some of these inclusions such as at Bo Rai in Thailand (Keller, 1990). The Barrington rubies show many similarities, except that they contain prevalent pleonaste and chromian pleonaste spinels among the mineral inclusions.

Ruby is considered the most valuable gemstone after fancy coloured diamonds and is far more valuable than sapphire, with very few sources producing facet-quality ruby in any quantity (Hughes, 1990). Thus, the Barrington ruby-bearing aggregates have implications for exploration, not only in Australia (Cluff Resources Pacific Ltd, 1993 Annual Report, Sydney), but also within Asian basaltic fields (Vichit, 1992). The presence of sapphirine (harder than quartz and with a S.G. of 3.46–3.49) in the aggregates raises its potential as an alluvial indicator mineral for ruby. Sapphirine is associated with ruby and other heavy minerals in

TABLE 6. Analyses, heavy minerals associated with ruby, Rubywell Mine, Thailand

Analysis (wt.%)	Garnet	Sapphirine	Ilmenite	Spinel	Pleonaste
SiO ₂	41.1–42.3	15.4–16.8			
TiO ₂	0.4–0.6		39.1–51.2	0.0–0.1	0.3–1.0
Al ₂ O ₃	22.6–23.4	60.7–62.6	0.6–1.3	65.2–67.4	57.7–60.5
Cr ₂ O ₃		0.2–0.4		0.3–1.4	
FeO Total	11.8–13.7	2.9–3.7	39.5–35.5	8.3–10.9	24.9–27.5
MnO	0.3–0.5		0.0–0.3		0.0–0.3
MgO	16.1–17.7	18.6–19.4	1.8–6.8	21.0–22.7	12.3–15.7
CaO	4.8–5.4	0.0–0.1			
NiO		0.0–0.5		0.0–0.7	
No. of analyses	9	5	10	3	2

Analyses: Autotech Electron Microprobe with Link EDS, Macquarie University, R.R. Coenraads.

gravels below fine clays and volcanic ash at the Rubywell Mine, in the Trat region of Thailand (R.R. Coenraads data; Table 6). However, the sapphirine and spinel mineral compositions in the Rubywell suite differ from those in the Barrington aggregates in Mg/Fe contents, supporting the suggestion that sapphirine indicators show regional compositional variations. The spinels have little worth as ruby indicators, as similar spinels are widespread within basaltic fields where sapphires predominate and ruby is rare, e.g. New England gemfields (Coenraads, 1990).

The present study of the Barrington gemfields suggests that corroded corundums have shed from basaltic hosts and form two distinct suites. One features well-formed crystals, blue-green colours and growth-banded colour zoning and contains Fe-rich spinels and common rutile/hematite exsolution among the inclusions. This suite dominates eastern Australian gemfields, where accompanying gem zircons commonly give fission track ages related to local basaltic eruptions (Sutherland and Wellman, 1986; Robertson and Sutherland, 1992; Sutherland *et al.*, 1993a,b). Mineral inclusions in these sapphires contain a variety of Large Ion Lithophile (U, Th) and High Field Strength (Zr, Nb, Hf, Ta) elements (Coenraads *et al.*, 1990; Coenraads, 1992). Fluid inclusions contain CO₂ and saline water and suggest origins at depths up to 10 kbar (Stephenson, 1990). Such sapphire suites also dominate many Thai and Chinese gemfields (Hughes, 1990; Guo *et al.*, 1992a) and different coloured sapphires intergrown with zircon crystals in an octahedral magnetite are recorded in a xenolith from the Chanthaburi field, Thailand (Coenraads *et al.*, 1995). Zircons that crystallized with such sapphires give U-Pb isotope ages matching local basalt ages (Coenraads *et al.*,

1990, 1995; Guo *et al.*, 1992b). There is some debate on the origin of these sapphires, as to whether they crystallize from alkaline felsic melts at upper mantle depths (Coenraads *et al.*, 1990, 1995), result from more complex interactions of alkaline and carbonatite magmas at mid-crustal levels? (Guo *et al.*, 1992a) or represent aluminous materials metamorphosed during ocean floor subduction (Levinson and Cook, 1995).

The unusual corundum suite described in this paper features heavily corroded, anhedral crystals showing only minor gradational zoning and a range of pastel colours. These include blue-purple rather than blue-green colours and also a range of pink to mauve colours, grading into ruby. Mineral inclusions are dominated by pleonaste spinels and exsolved rutile or hematite is rarely seen. These sapphires and rubies are derived from a corundum-sapphirine-spinel assemblage whose origin needs further characterization.

Contrasting corundum suites also contribute to the SE Asian 'volcanic' gemfields. The Chanthaburi-Trat gemfields in Thailand show geographic variation in gem corundum colours over a 80 km distance, passing from blue, green, yellow sapphires through blue green sapphires and rubies, into rubies (Vichit, 1992). On examining gem concentrates from the transitional region (R.R. Coenraads), it is clear that sapphires with larger, broken euhedral crystals form a different suite to the small, anhedral ruby crystals. This zone may thus represent an overlap of two distinct gem corundum sources. Pailin in western Kampuchea provides a further contrast (Berrangé and Jobbins, 1976) producing essentially blue sapphire (similar to the common eastern Australian type) in some sites, and ruby (similar to the Barrington type) in other sites, while other colour varieties, as found at

Barrington, are virtually absent (Jobbins and Berrangé, 1981; Hughes, 1990). Detailed comparisons between Australian and SE Asian gem corundum suites should provide a firmer consensus on the precise origins of rubies and sapphires in such volcanic gemfields.

Acknowledgements

The authors wish to thank A.W. Chubb of Gloucester who provided the raw materials and a continued interest in this study; C. Nockolds, Electron Microscope Unit, University of Sydney, for assistance with analytical work; G. Webb, R. Pogson and B.J. Barron, Mineralogy and Petrology Section, Australian Museum, for photography, inclusion studies and mineral calculations; P.J. Kennewell, Cluff Resources Pacific, Sydney and G.M. Oakes, New South Wales Department of Mineral Resources who provided additional ruby materials from the Barrington-Gloucester area for inspection and J.D. Hollis, Trentham, Victoria; W.D. Birch, Museum of Victoria and A.D. Robertson, Queensland Department of Resource Industries, who provided information on Australian ruby localities. K.A. Rodgers, Geology Department, University of Auckland kindly read the script and M.R. Fiske, College of Oceanography, Oregon State University, USA, provided information on experimental work. The Australian Museum Trust supported the study and S. Folwell typed the script.

References

- Barker, F. (1964) Reaction between mafic magmas and pelitic schist, Cortlandt, New York. *Amer. J. Sci.*, **262**, 614–34.
- Berrangé, J.P. and Jobbins, E.A. (1976) The Geology, Gemmology, Mining Methods and Economic Potential of the Pailin Ruby and Sapphire Gemfield, Khmer Republic. *Inst. Geol. Sci., Overseas Div. Rep.*, **35**, 32 pp.
- Bertrand, P., Ellis, D.J. and Green, D.H. (1991) The stability of sapphirine-quartz and hypersthene-sillimanite-quartz assemblages: an experimental investigation in the system FeO–MgO–Al₂O₃–SiO₂ under H₂O and CO₂ conditions. *Contrib. Mineral. Petrol.*, **108**, 55–71.
- Bishop, F.C. and Newton, R.C. (1975) The composition of low-pressure synthetic sapphirine. *J. Geol.*, **83**, 511–7.
- Coenraads, R.R. (1990) Key areas for alluvial diamond and sapphire exploration in the New England gem fields, New South Wales, Australia. *Econ. Geol.*, **85**, 1186–207.
- Coenraads, R.R. (1992) Sapphires and rubies associated with volcanic provinces: inclusions and surface features shed light on their origin. *Austral. Gemmol.*, **18**(3), 70–78.
- Coenraads, R.R., Sutherland, F.L. and Kinny, P.D. (1990) The origin of sapphires: U–Pb dating of zircon inclusions sheds new light. *Mineral. Mag.*, **54**, 113–22.
- Coenraads, R.R., Vichit, P. and Sutherland, F.L. (1995) An unusual sapphire-zircon-magnetite xenolith from the Chanthaburi Gem Province, Thailand. *Mineral. Mag.*, **59**, 465–79.
- Coldham, T. (1985) Sapphires from Australia. *Gems & Gemology*, **21**, 130–46.
- Collins, W.J., Offler, R., Farrell, J.R. and Landenberger, B. (1993) A revised Late Palaeozoic–Early Mesozoic tectonic history for the southern New England Fold Belt. In *New England Orogen, eastern Australia* (P.G. Flood and J.C. Aitchison, eds.), Dept. Geol. Geophys., Univ. New England, Armidale, N.S.W., pp 69–84.
- Deer, W.A., Howie, R.A. and Zussman, J. (1978) *Rock-Forming Minerals Single-Chain Silicates* Volume 2A Second Edition, Longman Group, London, 668 pp.
- Droop, G.T.R. (1987) A general equation for estimating Fe³⁺ concentrations in ferromagnesian silicates and oxides from microprobe analyses, using stoichiometric criteria. *Mineral. Mag.*, **51**, 431–5.
- Eggins, S. and Hensen, B.J. (1987) Evolution of mantle-derived, augite-hypersthene granodiorites by crystal-liquid fractionation: Barrington Tops Batholith, eastern Australia. *Lithos*, **20**, 295–310.
- Fisk, M.R. and Ford, C.E. (1984) Melting of Mauritius Island intermediate series lava. *Progress Exp. Petrol. (N.E.R.C.)*, **6**, 114–8.
- Griffin, W.L. and O'Reilly, S.Y. (1986) Sapphirine in a mantle-derived xenolith from Delegate, Australia. *Mineral. Mag.*, **50**, 635–40.
- Gübelin, E.J. and Koivula, J.I. (1986) *Photo atlas of inclusions in gemstones*, ABC Edition, Zurich, 531 pp.
- Guo, J.F., O'Reilly, S.Y. and Griffin, W.L. (1992a) Origin of sapphire in eastern Australian basalts: Inferred from inclusion studies. *Geol. Soc. Austral. Abstr. Ser.*, **32**, 219–20.
- Guo, J., Wang, F. and Yakoumelos, G. (1992b) Sapphires from Changle in Shandong Province, China. *Gems & Gemology*, **28**, 255–60.
- Hensen, B.J. (1986) Theoretical phase relations involving cordierite and garnet revisited: the influence of oxygen fugacity on the stability of sapphirine and spinel in the system Mg–Fe–Al–Si–O. *Contrib. Mineral. Petrol.*, **92**, 362–7.
- Hughes, R.W. (1990) *Corundum*, Butterworth-Heinemann, London, 314 pp.
- Jobbins, E.A. and Berrangé, J.P. (1981) The Pailin ruby and sapphire gemfield, Cambodia. *J. Gemmol.*, **17**, 555.

- Johnson, R.W., compl. and ed. (1989) *Intraplate Volcanism in Eastern Australia and New Zealand*, Cambridge University Press, Cambridge, 408 pp.
- Keller, P.C. (1990) *Gemstones and their Origins*, Van Nostrand Reinhold, New York, 144 pp.
- Keller, P.C. (1992) *Gemstones of East Africa*, Geoscience Press, Phoenix, Arizona, 144 pp.
- Kimbrough, D.L., Cross, K.C. and Korsch, R.J. (1993) U-Pb isotopic ages for zircons from the Pola Fogal and Nundle granite suites, southern New England Orogen. In: *New England Orogen, eastern Australia* (P.G. Flood and J.C. Aitchison, eds), Dept. Geol. Geophys., Univ. New England, Armidale, N.S.W., 403–12.
- Koivula, J.I. and Fryer, C.W. (1987) Sapphirine (not sapphire) in a ruby from Bo Rai, Thailand. *J. Gemmol.*, **20**, 369–70.
- Levinson, A.A. and Cook, F.A. (1995) Gem corundum in alkali basalt: Origin and occurrence. *Gems & Gemology*, **30**, 253–62.
- Lindsley, D.H. (1976) Experimental studies of oxide minerals. In: *Oxide Minerals* (D. Rumble ed.), Res. Mineral., Mineral. Soc. Am., vol 3, 61–88.
- Liu, T.-C. and Presnall, D.C. (1990) Liquidus phase relationships on the join anorthite-forsterite-quartz at 20 kbar with applications to basalt petrogenesis and igneous sapphirine. *Contrib. Mineral. Petrol.*, **104**, 735–42.
- MacNevin, A.A. (1977) Diamonds in New South Wales. *Dept. Min. Geol. Surv. NSW. Miner. Resour.*, **42**, 125 pp.
- MacNevin, A.A. and Holmes, G.G. (1980) Gemstones. *Geol. Surv. NSW., Miner. Indus. N.S.W.*, **18**, 119 pp.
- Mason, D.R. (1982) Stratigraphy of western parts of the Barrington Tops Tertiary volcanic field. In: *New England Geology, A. H. Voisey Symposium* (P.G. Flood and B. Runnegar, eds), Dept. Geol. Univ. New England & A. H. V. Club, Armidale, N.S.W., 133–9.
- Mason, D.R. (1989) Barrington. In: *Intraplate Volcanism in eastern Australia and New Zealand* (R.W. Johnson, compl. and ed.), Cambridge University Press, Cambridge, 123–4.
- McBirney, A.R. and Hunter, R.H. (1995) The cumulate paradigm reconsidered. *J. Geology*, **103**, 114–22.
- Mountain, E.D. (1939) Sapphirine crystals from Blinkwater, Transvaal. *Mineral. Mag.*, **25**, 277–82.
- Oliver, G.J. and Townsend, I.J. (1993) *Gemstones in Australia*, Australian Gemstone Industry Council, 72 pp. Australian Government Publishing Service, Canberra.
- O'Reilly, S.Y., Griffin, W.L. and Stabel, A. (1988) Evolution of Phanerozoic eastern Australia: isotopic evidence for magmatic and tectonic underplating. In: *Oceanic and Continental Lithosphere: Similarities and Differences* (M.A. Menzies and K.G. Cox, eds). *J. Petrol.-Special Publ.*, 89–108.
- Owen, J.V. and Greenough, J.D. (1991) An empirical sapphirine-spinel Mg-Fe exchange thermometer and its application to high grade xenoliths in the Pope Harbour dyke, Nova Scotia, Canada. *Lithos*, **26**, 317–32.
- Pain, C.F. (1983) Geomorphology of the Barrington Tops area, New South Wales. *J. Geol. Soc. Austral.*, **30**, 187–94.
- Robertson, A.D. and Sutherland, F.L. (1992) Possible origins and ages for sapphire and diamonds from the Central Queensland gemfields. In: *R. O. Chalmers Commemorative Papers (Mineralogy, Meteorites, Geology)* (F.L. Sutherland, ed). *Rec. Austral. Museum Suppl.*, **15**, 45–54.
- Rock, N.M.S. (1991) *Lamprophyres*, Van Nostrand Reinhold, New York, USA, 285 pp.
- Smart, R.M. and Glasser, F.P. (1976) Phase relationships of cordierite and sapphirine in the system MgO-Al₂O₃-SiO₂. *J. Mater. Sci.*, **11**, 1459–64.
- Stephenson, P.J. (1990) The geological context of sapphire occurrences in the Anakie region, central Queensland. *Geol. Soc. Austral. Abstr. Ser.*, **25**, 232–3.
- Sutherland, F.L. (1985) Regional controls in Eastern Australian volcanism. In: *Volcanism in Eastern Australia with case histories from New South Wales* (F.L. Sutherland, B.J. Franklin and A.E. Walther, eds), *Geol. Soc. Austral., New South Wales Div. Publ.*, **1**, 13–31.
- Sutherland, F.L. (1991) *Gemstones of the Southern Continents*, Reed Books, Sydney, 256 pp.
- Sutherland, F.L. and Wellman, P. (1986) Potassium-argon ages of Tertiary volcanic rocks, Tasmania. *Pap. Proc. Roy. Soc. Tasm.*, **120**, 77–86.
- Sutherland, F.L., Barron, B.J. and Webb, G.B. (1993a) Barrington volcano-repeated gemstone eruptions (zircon, sapphire and ruby) at the edge of the Sydney Basin. *Adv. Stud. Syd. Bas.*, **26th Newcastle Symp. Proc.**, 137–44.
- Sutherland, F.L., Pogson, R.E. and Hollis, J.D. (1993b) Growth of the central New England basaltic gemfields, New South Wales, based on zircon fission track dating. In: *New England Orogen, eastern Australia* (P.G. Flood and J.C. Aitchison, eds), *Dept. Geol. Geophys.*, Univ. New England, Armidale, N.S.W., 483–91.
- Taylor, H.C.J. (1973) Melting relations in the system MgO-Al₂O₃-SiO₂ at 15 kb. *Bull. Geol. Soc. Amer.*, **84**, 1335–48.
- Vernon, R.H. (1970) Comparative grain-boundary studies of some basic and ultrabasic granulites, nodules and cumulates. *Scottish J. Geol.*, **6**, 337–51.
- Vichit, P. (1992) Gemstones in Thailand. In: *Proceedings of the National Conference on "Geologic Resources of Thailand: Potential for Future Development"* (C. Piencharoen, ed. in chief), Dept. Mineral Resources, Bangkok, Thailand, 124–50.

- Wellman, P. (1989) Upper Mantle, Crust and Geophysical Volcanology of Eastern Australia. In: *Intraplate Volcanism in Eastern Australia and New Zealand* (R. W. Johnson, compl. and ed.), Cambridge University Press, Cambridge, 29–38.
- Wellman, P. and McDougall, I. (1974) Potassium-argon ages of the Cainozoic volcanic rocks of New South Wales, Australia. *Geol. Soc. Austral.*, **21**, 247–72.
- [Manuscript received 23 March 1995:
revised 24 July 1995]